Journal of Solid State Chemistry 181 (2008) 1634–1641

Contents lists available at ScienceDirect

Journal of Solid State Chemistry

journal homepage: www.elsevier.com/locate/jssc

GaN taper rods: Solid-phase synthesis, crystal defects, and optical properties

Keyan Bao, Shuzhen Liu, Liang Shi, Shenglin Xiong, Jun Li, Xiaobo Hu, Jie Cao, Yitai Qian *

Hefei National Laboratory for Physical Sciences at Microscale, Department of Chemistry, University of Science and Technology of China, Hefei, Anhui 230026, PR China

ARTICLE INFO

Article history:
Received 12 April 2008
Received in revised form
30 May 2008
Accepted 2 June 2008
Available online 5 June 2008

Keywords:
GaN
Taper rods
Precursor template
GaOOH
$NaNH_2$

ABSTRACT

Wurtzite GaN taper rods assembled from highly oriented nanoparticles were synthesized using $NaNH_2$ and the as-synthesized GaOOH prismatic rods as reactants at 600 °C for 5 h. The lengths of the GaN taper rods are in the range of 4–6 μm and the diameters are about 0.5–1.5 μm. It was found that a slow heating rate (1 °C min^{-1}) was beneficial to keeping the one-dimensional (1D) skeleton of GaN, otherwise only GaN nanoparticles were obtained with a quick heating rate (10 °C min^{-1}). Selected area electron diffraction (SAED) patterns and high-resolution transmission electron microscopy (HRTEM) observations revealed that the GaN taper rods assembled from highly oriented nanoparticles and there were crystal defects in the GaN structure. The GaN taper rods displayed luminescence emission in the blue-violet region, which may be related to crystal defects.

1. Introduction

GaN, an important III–V semiconductor with a direct band gap of 3.39 eV at room temperature, has a wide use in optical devices operating at blue and ultraviolet wavelengths and in high-temperature electronic devices [1,2]. Up to now, many structures of GaN such as nanoparticles [3–8], nanowires [9–13], nanorods [14–16], nanobelts [17], hollow spheres (spindles) [18], and tubes [19–23] have been successfully synthesized.

Many reports showed that the shapes, sizes, and crystalline structures of semiconductors could greatly affect their physical and chemical properties [24,25]. One-dimensional (1D) nanomaterials, such as naowires, nanorods, and nanobelts [26–29], exhibit lots of special properties in optical, electrochemical, mechanical, and thermal facets. At present, the controlled synthesis of 1D nanomaterials has attracted much attention. In detail, 1D structure of GaN has been grown by many methods, such as chemical vapor deposition [30], metal-organic chemical vapor deposition [31], molecular beam epitaxy [32], halide vapor-phase epitaxy [33], arc discharge [34], magnetron sputtering [35], chemical thermal-evaporation process [36], etching [37], and ammonolysis [38–41].

Recently, the precursor-templated method has been applied to synthesize many micro- or nanostructures of materials such as Ag and CdS microcages [42,43], CdS and CuS nanotubes [44,45]. Inspired by the above reports, we extend the precursor-templated method here to prepare wurtzite GaN taper rods, which assembled from highly oriented nanoparticles. The synthesis of wurtzite GaN taper rods involved two steps: first, hydrothermal synthesis of GaOOH prismatic rods at 200 °C for 24 h; second, preparation of GaN taper rods using $NaNH_2$ and the as-prepared GaOOH prismatic rods as reactants at 600 °C for 5 h.

2. Experiment section

2.1. Synthesis of GaOOH prismatic rods

In a typical synthesis, 0.7 g (10 mmol) of commercial Ga (99.99%) was dissolved in 5 mL concentrated nitric acid to form a clear solution. After evaporation, 25 mL of deionized water was added. Then 5 mL of diluted ammonia water was introduced to the solution under vigorous stirring till the pH value reached 8.8. The as-obtained colloidal precipitate was transferred into a 50 mL Teflon-lined autoclave. The autoclave was sealed, maintained at 200 °C for 24 h, and then allowed to cool to room temperature naturally. The resulting white precipitate was retrieved by centrifugation, washed several times with distilled water and absolute ethanol, and dried under vacuum at 60 °C for 8 h.

2.2. Preparation of GaN taper rods

In total, 1.03 g (10 mmol) of the as-prepared GaOOH prismatic rods and 0.63 g (16 mmol) of $NaNH_2$ were mixed and then put into

* Corresponding author. Fax: +86 551 3607402.
E-mail address: ytqian@ustc.edu.cn (Y. Qian).

0022-4596/$ - see front matter © 2008 Published by Elsevier Inc.
doi:10.1016/j.jssc.2008.06.002

a stainless steel autoclave. The autoclave was heated to 600 °C with the heating rate of 1 °C min^{-1}, maintained at 600 °C for 5 h and then cooled to room temperature naturally. A yellow powder was retrieved by centrifugation, washed several times with dilute hydrochloric acid, distilled water and absolute alcohol, and finally dried in a vacuum oven at 60 °C for 8 h.

2.3. Characterization

Powder X-ray diffraction (XRD) measurements were carried out with a Philips X'Pert diffractmeter (Cu$K\alpha$ $\lambda = 1.541874$ Å; nickel filter; 40 kV, 40 mA). Field emission scanning electron microscope (FESEM) images were taken on a JEOL JSM-6300F SEM. Transmission electron microscopy (TEM) images, high-resolution transmission electron microscopy (HRTEM) ages and selected area electron diffraction (SAED) were performed on JEOL JEM-2010 microscope operating at 200 kV. The Raman spectrum was obtained on the JY LABRAM-HR laser micro-Raman spectrometer with 514.5 nm emission lines. Photoluminescence (PL) measurements were carried out on a Perkin-Elmer LS-55 luminescence spectrometer using a pulsed Xe lamp.

3. Results and discussion

3.1. Characterization of GaOOH prismatic rods

GaOOH prismatic rods were synthesized through a hydrothermal process at 200 °C for 24 h. The product was characterized by XRD and was found to be orthorhombic phase of GaOOH (JCPDS PDF no. 26-0674, $a = 4.5$ Å, $b = 9.75$ Å, $c = 2.97$ Å) (see Fig. SI-1, Supplementary Information). Figs. 1a and b show the FESEM and TEM images of the as-prepared GaOOH. As shown in the images, the GaOOH prismatic rods have smooth faceted surfaces, diameters in the range of 200–400 nm and length of about 4–5 μm. Further information about the microstructure of the as-synthesized GaOOH prismatic rods was provided by HRTEM image and SAED pattern. Fig. 1c exhibits the HRTEM image obtained from the oblong region marked c in Fig. 1b. The HRTEM image reveals that the crystal planes have lattice spacing of about 0.253 nm corresponding to (021) plane of orthorhombic GaOOH. The corresponding SAED pattern (Fig. 1d) also indicates that the as-prepared GaOOH is single crystal and the SAED spots can be indexed as orthorhombic GaOOH (001), (021), and (020) planes.

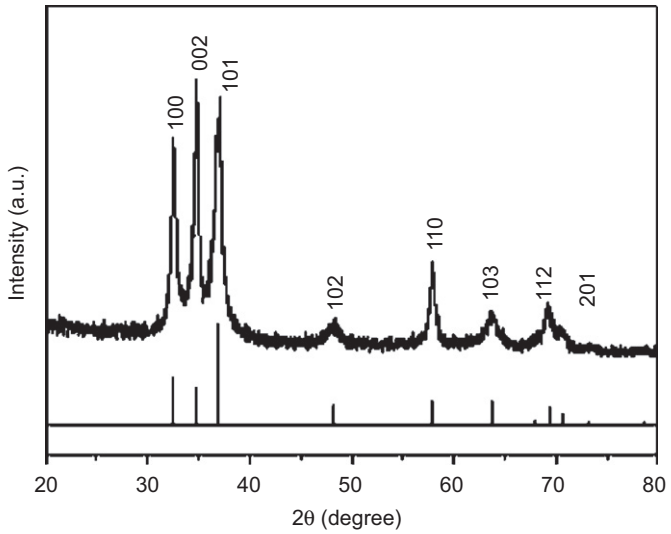

Fig. 2. The XRD pattern of the as-prepared GaN product synthesized at 600 °C for 5 h. The bars show the position and intensity of diffraction peaks from the Joint Committee on Powder Diffraction Standards file no. 74-0243 for wurtzite GaN.

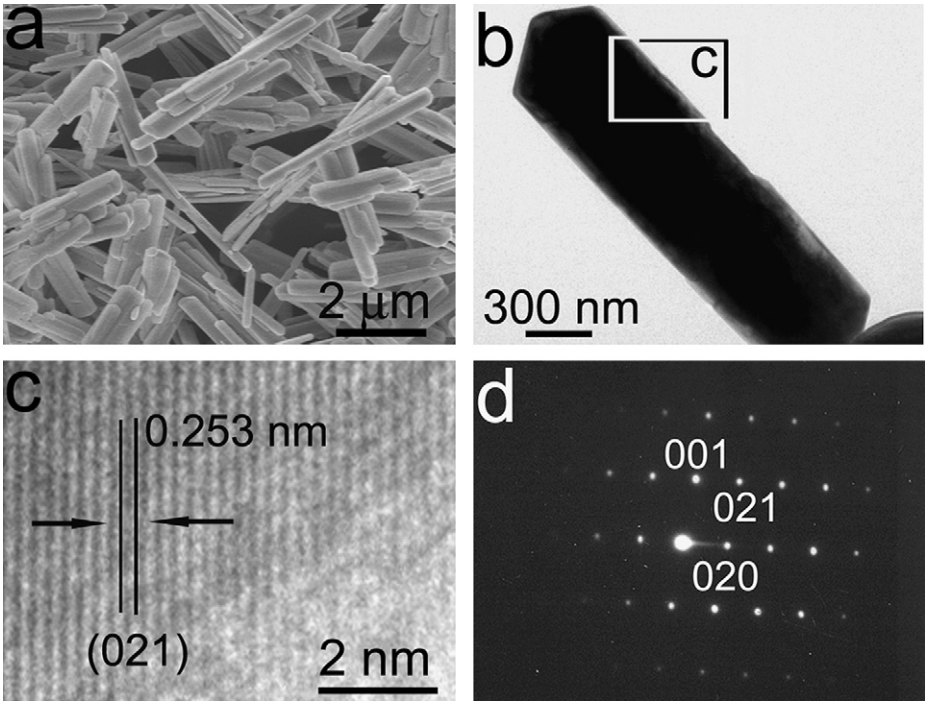

Fig. 1. (a) FESEM image, (b) TEM image, (c) HRTEM image obtained from the oblong region labeled c in Fig. 1b, and (d) corresponding SAED pattern of the as-prepared GaOOH prismatic rods.

3.2. Characterization of GaN taper rods

The GaN taper rods were prepared via a solid-state reaction using $NaNH_2$ and the as-prepared GaOOH prismatic rods as reactants in a stainless steel autoclave. The autoclave was heated to 600 °C with a speed of 1 °C min^{-1} and maintained at 600 °C for 5 h. Fig. 2 indicates the XRD pattern of the as-prepared product. All the reflection peaks can be indexed as wurtzite GaN, which is in good agreement with the standard data (JCPDS PDF no. 74-0243, $a = 3.195$ Å, $c = 5.182$ Å). The XRD pattern shows a much stronger 0 0 2 peak relative to the 1 0 0 and 1 0 1 peaks, because the rods were laid horizontally (parallel to the substrate) or close to horizon when the XRD pattern was taken—and due to the fact that the rods structure were made of highly oriented GaN nanocrystals. The below HRTEM and SAED analysis also confirm the opinion.

The GaN taper rods were synthesized on a large scale, as revealed in Fig. 3a where a panoramic FESEM image of the product is displayed. Fig. 3b presents a middle magnification FESEM image of the product, exhibiting that the lengths of the taper rods are in the range of 4–5 μm and about 0.5–1.5 μm in diameters. The high-magnification FESEM image (Fig. 3c) also indicates that the taper rods have rather rough surfaces which consist of densely packed GaN nanoparticles about 100–200 nm. Fig. 3d is a representative TEM image of GaN taper rods, displaying that the product is solid structure. The triangular segment in Fig. 3d was further investigated by SAED and HRTEM and the images are shown in Fig. 4.

Fig. 4a presents the high-magnification TEM image of the segment marked in Fig. 3d, revealing that the GaN architecture is constructed by small nanoparticles and those nanoparticles appear to be certain oriented. Fig. 4b is the SAED pattern taken from the oblong region marked in Fig. 4a and the SAED spots can be indexed as wurtzite GaN $(10\bar{1}0)$ $(01\bar{1}0)$, and $(\bar{1}100)$ planes of wurtzite GaN. Fig. 4c is the HRTEM image also obtained from the oblong region marked in Fig. 4a, displaying that the overlap section of two nanoparticles where the crystal planes are still continuous. The clearly resolved interplanar distances are all measured to be 0.275 nm, corresponding to the $(10\bar{1}0)$ and $(01\bar{1}0)$ crystal planes of wurtzite GaN. The separation angle between them is measured at 60°. The SAED and HRTEM results confirm that GaN taper rods consist of densely packed GaN nanoparticles.

The structure of a single GaN nanoparticle was also investigated by HRTEM. Fig. 5a is the TEM image of a single GaN nanoparticle. Fig. 5b is the HRTEM image obtained from the region labeled b in Fig. 5a. Careful observation from the HRTEM image reveals that the pinstripes in the regions labeled d and e are much more disordered than that in the region marked with c. The regions labeled c, d, e are all magnificated and the images are shown in Figs. 5c–e, respectively. Fig. 5c displays the crystal planes have lattice spacing of about 0.275 nm corresponding to the $(10\bar{1}0)$ plane of wurtzite GaN. However, Figs. 5d and e indicate that the pinstripes are not continuous and some of them have been distorted. This is to say there are crystal defects in GaN structure.

Further study shows that heating rate has a dramatic effect on morphologies of the GaN products. Figs. 6a–c exhibit the FESEM images of the products synthesized at 600 °C for 5 h with different heating rate. As shown in Fig. 6a, when the heating rate was 1 °C min^{-1}, GaN taper rods assembled from small nanoparticles about 100 nm were obtained. Fig. 6b displays the FESEM image of the sample prepared with the heating rate of 2 °C min^{-1}, revealing that the product was a cylinder rod assembled from nanoparticles about 200 nm. The morphology of GaN turned into nanoparticles when the heating rate was increased to 10 °C min^{-1}, as shown in Fig. 6c. Fig. 6d exhibits the XRD patterns of the three products obtained with different

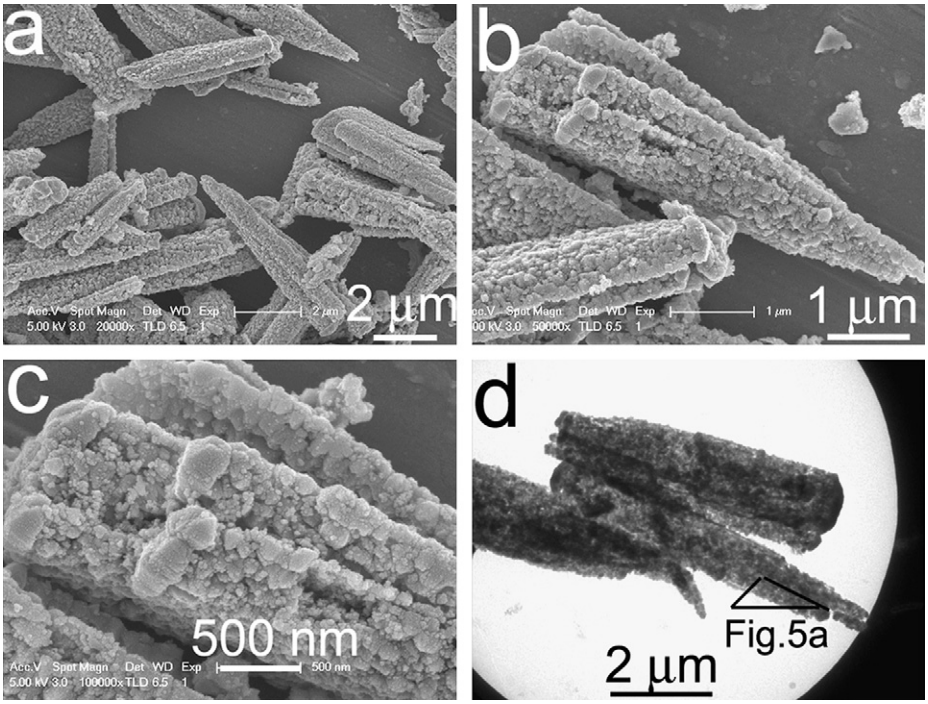

Fig. 3. FESEM images of GaN taper rods at (a) low, (b) middle, and (c) high magnification. (d) TEM image of GaN taper rods. The segment in the triangular section was enlarged and shown in Fig. 4a.

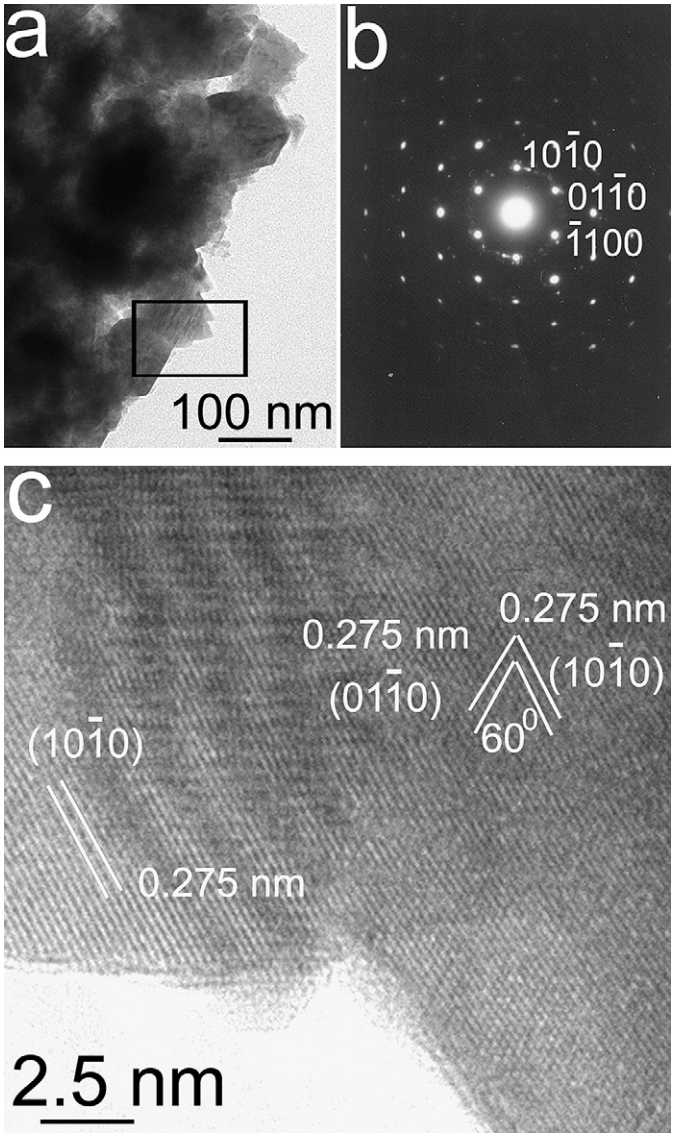

Fig. 4. (a) High-magnification TEM image of the segment recorded in Fig. 3d, (b) SAED pattern, and (c) HRTEM image obtained from the oblong region marked in Fig. 4a.

heating rate, indicating that the product synthesized at a slow heating rate (1 °C min^{-1}) shows a much stronger 0 0 2 peak relative to the 1 0 0 and 1 0 1 peaks. However, the XRD patterns of the other two products prepared with high heating rate (2 and 10 °C min^{-1}) do not appear that characteristic. The FESEM and XRD results suggest that a slow heating rate is beneficial to keeping the 1D framework of GaN and highly oriented of the nanoparticles on the surfaces.

To understand the growth mechanism of the GaN taper rods, several experiments were carried out at 600 °C with different lengths of time. The XRD patterns of the products are shown in Fig. 7. At 600 °C for 10 min and 1 h, the products were rhombohedral structure of Ga_2O_3 (JCPDS PDF no. 74-1610, $a = 4.98$ Å, $c = 13.43$ Å) and rhombohedral Ga_2O_3 with minor amount of wurtzite GaN, respectively (Figs. 7a and b). Pure GaN could be obtained at 600 °C for 3 and 5 h, as shown in Figs. 7c and d. The XRD results indicate that the as-prepared GaOOH prismatic rods first converted to rhombohedral Ga_2O_3 and then to wurtzite GaN.

The four samples were further investigated by FESEM. As shown in Fig. 8a, when the reaction was processed at 600 °C for 10 min, 1D skeleton of Ga_2O_3 with relatively smooth surfaces were obtained. When the reaction time was increased to 1 h, the sample was a mixture of Ga_2O_3 and GaN. The FESEM image (Fig. 8b) indicates that product consists of prismatic rods with nearly smooth surfaces and cylinder rods with rather rough surfaces. Pure GaN could be obtained at 600 °C for 3–5 h. Fig. 8c displays the FESEM image of the sample reacting for 3 h, revealing that GaN cylinder rods assembled from small nanoparticles were formed. When the reaction time was prolonged to 5 h, GaN taper rods with well-aligned nanoparticles were observed, as shown in Fig. 8d.

It is clear that the formation of GaN taper rods involves two steps: first, the orthorhombic GaOOH prismatic rods decomposed into rhombohedral Ga_2O_3 prismatic rods below 600 °C. Then the Ga_2O_3 prismatic rods transformed into GaN taper rods through a high-temperature reaction process without destroying the 1D framework. Based on the above discussion, the possible formation process could be suggested as follows:

$$2GaOOH\ Ga_2O_3 + H_2O \quad (1)$$

$$Ga_2O_3 + 3\ NaNH_2\ 2GaN + 3NaOH + NH_3 \quad (2)$$

The experimental results reveal that the reaction temperature plays a significant role in the formation of GaN. When the reaction temperature is lower than 500 °C, the product is Ga_2O_3 instead of wurtzite GaN. All the XRD reflection peaks can be indexed to orthorhombic Ga_2O_3 (see Fig. SI-2, Supplementary Information). Fig. 9a shows a panoramic FESEM image of the as-obtained Ga_2O_3, revealing that the prismatic rods have nearly smooth surfaces with diameters in the range of 250–450 nm and length of about 4–5 μm. Fig. 9b presents a high-magnification FESEM image of a single Ga_2O_3 rod, indicating that there are some cavities in the surface but the rod still preserves the prismatic structure. Fig. 9c exhibits a representative TEM image of a single Ga_2O_3 rod and the inset is the corresponding SAED pattern, which indicates that the Ga_2O_3 rod is a single crystal. Fig. 9d is the HRTEM image, which also confirms that the product is single crystal. The crystal planes have lattice spacings of about 0.363 and 0.411 nm corresponding to the $(1\bar{1}02)$ and $(10\bar{1}1)$ crystal planes of orthorhombic Ga_2O_3. If further decreasing the reaction temperature to 300 °C, the Eq. (1) cannot occur and the sample is still orthorhombic phase of GaOOH.

4. Optical properties measurement

Fig. 10 is the Raman spectrum of the as-prepared GaN taper rods. The spectrum clearly indicates that Raman peaks appear at 251, 410, 567, and 715 cm^{-1}. The first-order modes at 567 and 715 cm^{-1} exhibit the feature of red-shifts and broadening compared with the bulk GaN, which is attributed to the nanometer size effect [2]. The second-order Raman modes at 251 and 410 cm^{-1} are assigned to the zone-boundary phonon, activated by crystal defects and finite size effects, and the acoustic overtone of wurtzite GaN [13,14].

Fig. 11 shows the room temperature PL spectrum of the GaN taper rods recorded with excitation wavelength of 280 nm. The PL spectrum exhibits a broad emission band in the range of 420–450 nm, and the top of the emission peak separates into two peaks located at 427 and 444 nm, respectively. The broadband emission may be attributed to optical transitions from a shallow donor to a deep acceptor. The position of the PL band is related to a point defect [15,46]. The separation of the emission peak may be

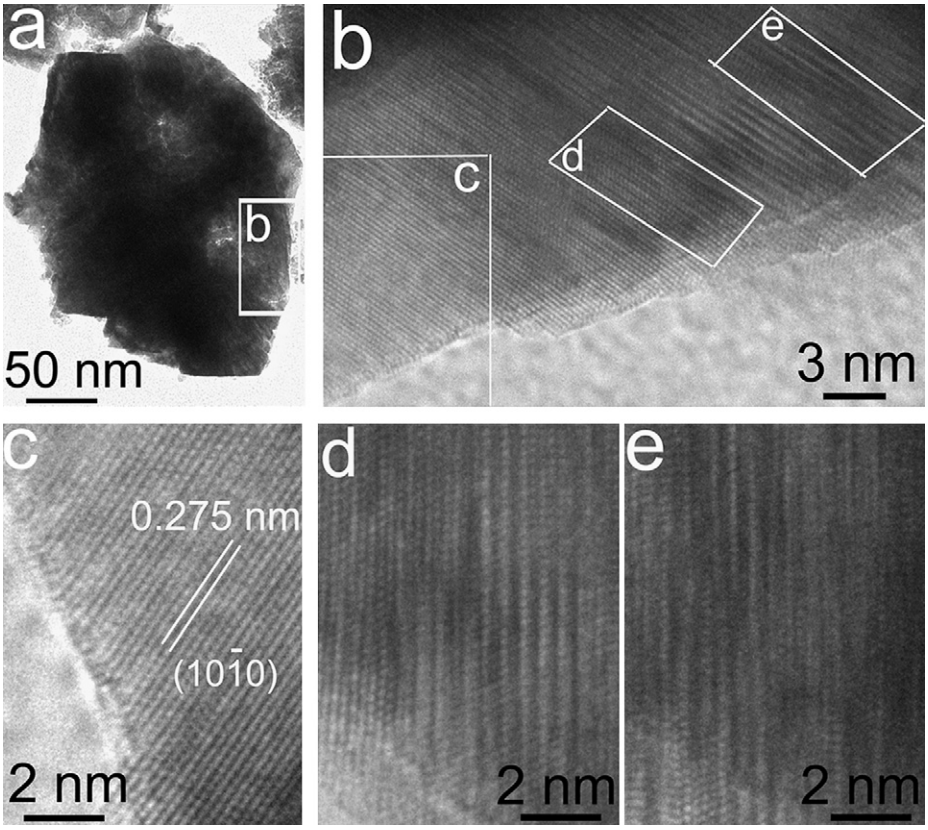

Fig. 5. (a) TEM image and (b) HRTEM image obtained from the oblong region labeled b in Fig. 5a. (c,d,e) high-magnification HRTEM images obtained from the oblong regions labeled c–e in Fig. 5b.

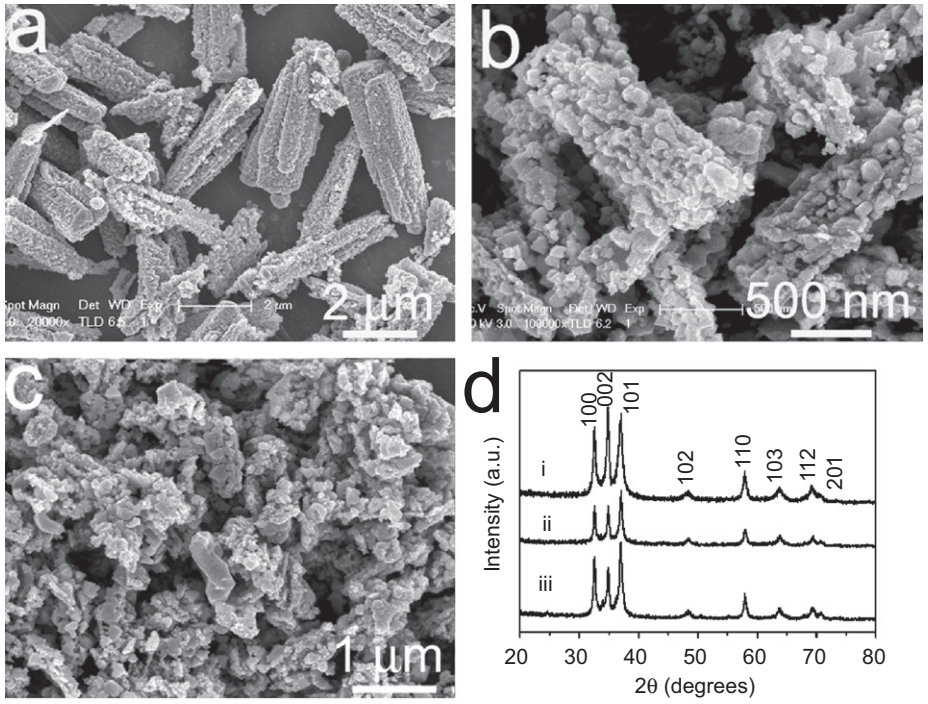

Fig. 6. FESEM images of the GaN products synthesized at 600 °C for 5 h with different heating rate (a) 1 °C min^{-1}, (b) 2 °C min^{-1}, (c) 10 °C min^{-1}, (d) i, ii, and iii are the XRD patterns of the products shown in (a)–(c), respectively.

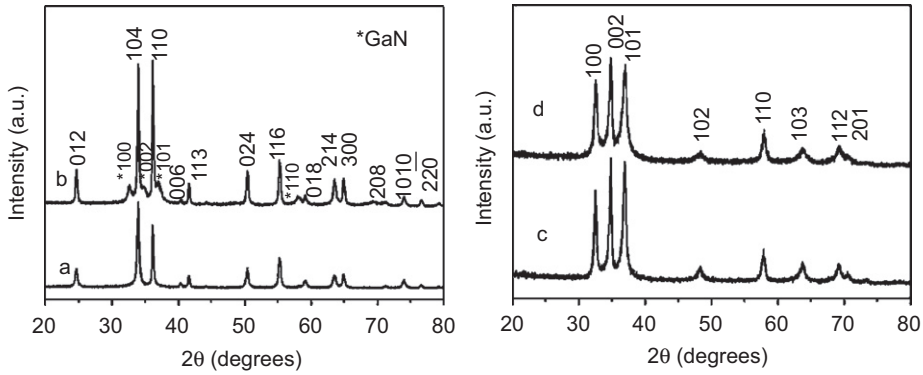

Fig. 7. The XRD pattern of the products obtained at 600 °C with heating rate of 1 °C min^{-1} for different reaction time (a) 10 min, (b) 1 h, (c) 3 h, and (d) 5 h. The small reflection peaks marked with asterisks * in Fig. 6b can be indexed as 1 0 0, 0 0 2, and 1 0 1 planes of wurtzite GaN.

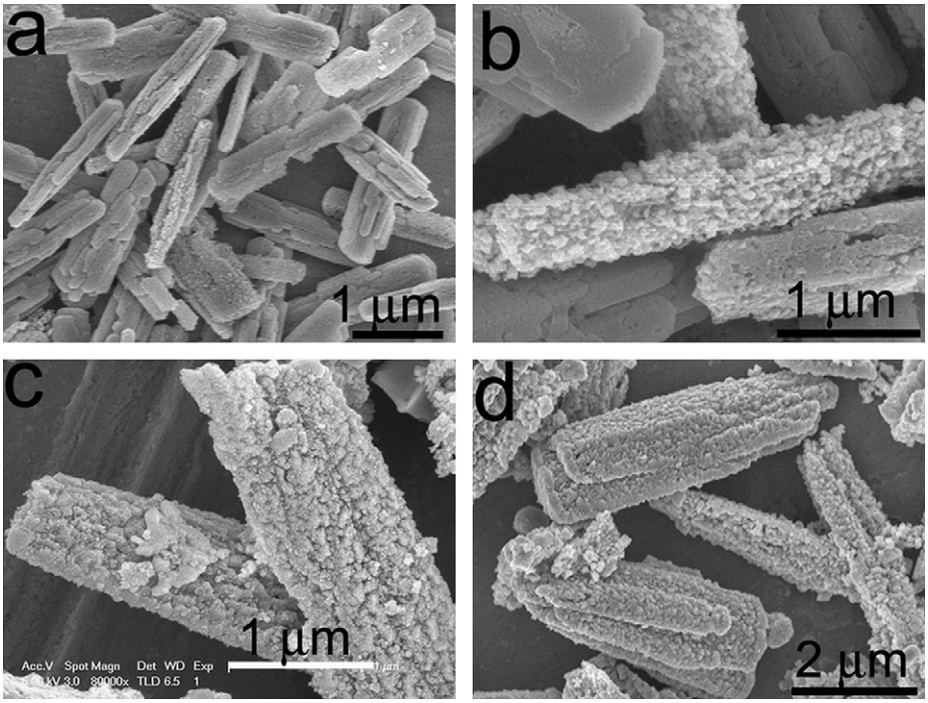

Fig. 8. FESEM images of the products obtained at 600 °C with heating rate of 1 °C min^{-1} for different reaction time (a) 10 min, (b) 1 h, (c) 3 h, and (d) 5 h.

due to the existence of the crystal defects, such as point defects, dislocations, and grain boundaries in the as-obtained GaN product [47,48]. The PL and Raman spectra indicate that the as-synthesized GaN taper rods have crystal defects, which agrees with the HRTEM observations. The crystal defects in the GaN taper rods can directly serve as radiative centers, which may be helpful for electro-optical applications of GaN material.

5. Conclusions

GaOOH prismatic rods have been transformed into GaN taper rods through a high-temperature reaction process in a stainless steel autoclave without destroying the 1D framework. The autoclave was heated with a speed of 1 °C min^{-1} and maintained at 600 °C for 5 h. It was found that rhombohedral Ga_2O_3 was the intermediate between the starting GaOOH precursor and the final GaN product. Experimental results demonstrated that a slow heating rate (1 °C min^{-1}) was beneficial to keeping the 1D skeleton of Ga_2O_3 and the 1D framework of GaN. SAED patterns and HRTEM observations revealed that the GaN taper rods were composed of highly oriented nanoparticles. Meanwhile, there were defects existence in the GaN structure and they could serve as radiative centers, which may be helpful for electro-optical applications of GaN material.

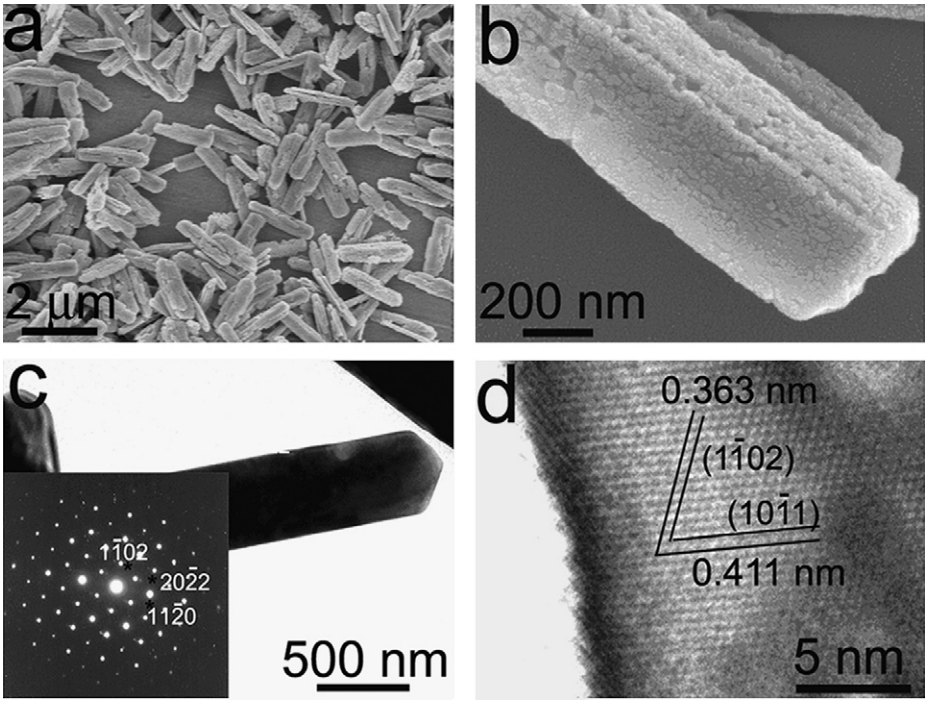

Fig. 9. (a) Low-magnification SEM image, (b) high-magnification SEM image, (c) TEM image and corresponding SAED pattern, (d) HRTEM image of orthorhombic Ga_2O_3 obtained at 500 °C for 8 h.

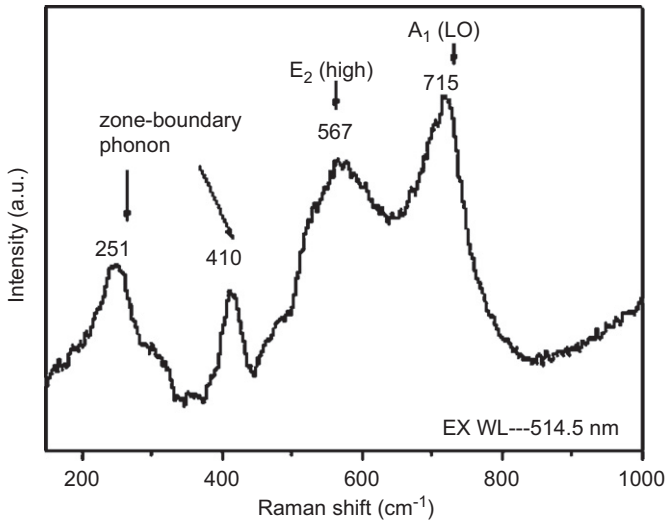

Fig. 10. Raman spectrum of the as-prepared GaN taper rods.

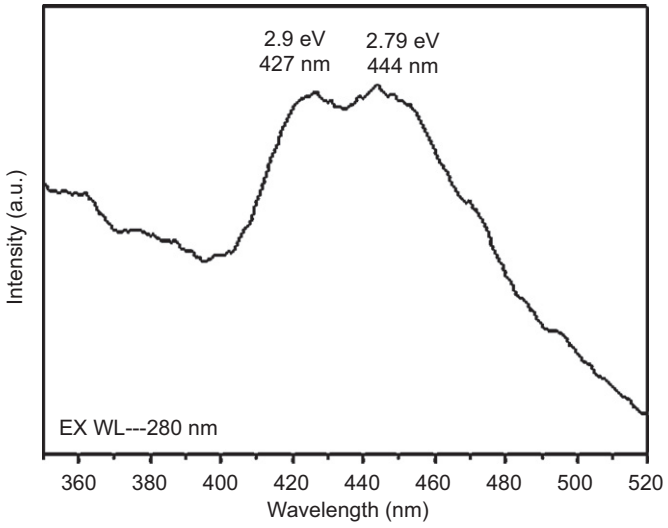

Fig. 11. Room-temperature photoluminescence (pL) spectrum of the as-prepared GaN taper rods.

Acknowledgments

The authors are thankful to Prof. Shuyuan Zhang for helpful discussions. The financial support of this work, by the China Postdoctoral Science Foundation (no. 20070420124), National Natural Science Foundation of China (no. 20431020) and the 973 Project of China (no. 2005CB623601), is gratefully acknowledged.

Appendix A. Supplementary materials

Supplementary data associated with this article can be found in the online version at doi:10.1016/j.jssc.2008.06.002.

References

[1] S. Nakamura, Nature 281 (1998) 956.
[2] B. Ha, S.H. Seo, J.H. Cho, C.S. Yoon, J. Yoo, G.C. Yi, C.Y. Park, C.J. Lee, J. Phys. Chem. B 109 (2005) 11095.
[3] S. Cho, J. Lee, I.Y. Park, S.T. Kim, Mater. Sci. Eng. B 95 (2002) 275.
[4] K. Sardar, C.N.R. Rao, Adv. Mater. 16 (2004) 425.
[5] Y. Xie, Y.T. Qian, W.Z. Wang, S.Y. Zhang, Y.H. Zhang, Science 272 (1996) 1926.
[6] F. Xu, Y. Xie, X. Zhang, S.Y. Zhang, L. Shi, New J. Chem. 27 (2003) 565.
[7] J.Q. Hu, B. Deng, W.X. Zhang, K.B. Tang, Y.T. Qian, Chem. Phys. Lett. 351 (2002) 229.
[8] S. Bhaviripudi, J. Qi, E.L. Hu, A.M. Belcher, Nanoletters 7 (2007) 3512.
[9] T. Kuykendall, P.J. Pauzauskie, Y.F. Zhang, J. Goldberger, D. Sirbuly, J. Denlinger, P.D. Yang, Nat. Mater. 3 (2004) 524.
[10] R. Calarco, R.J. Meijers, R.K. Debnath, T. Stoica, E. Sutter, H. Luth, Nanoletters 7 (2007) 2248.
[11] B.D. Liu, Y. Bando, C.C. Tang, F.F. Xu, D. Golberg, J. Phys. Chem. B 109 (2005) 21521.
[12] S.D. Hersee, X.Y. Sun, X. Wang, Nanoletters 6 (2006) 1808.
[13] C.C. Chen, C.C. Yeh, C.H. Chen, M.Y. Yu, H.L. Liu, J.J. Wu, K.H. Chen, L.C. Chen, J.Y. Peng, Y.F. Chen, J. Am. Chem. Soc. 123 (2001) 2791.
[14] J.K. Jian, X.L. Chen, Q.Y. Tu, Y.P. Xu, L. Dai, M.J. Zhao, Phys. Chem. B 108 (2004) 12024.
[15] S.Y. Bae, H.W. Seo, J. Park, H.N. Yang, H. Kim, S. Kim, Appl. Phys. Lett. 82 (2003) 4564.
[16] X. Xiang, H. Zhu, Appl. Phys. A 87 (2007) 651.
[17] X. Xiang, C.B. Cao, H. Zhu, Solid State Commun. 126 (2003) 315.
[18] X.M. Sun, Y.D. Li, Angew. Chem. Int. Ed. 43 (2004) 3827.
[19] J. Goldberger, R.R. He, Y.F. Zhang, S.W. Lee, H.Q. Yan, H.J. Choi, P.D. Yang, Nature 422 (2003) 599.
[20] J.Q. Hu, Y. Bando, D. Golberg, Q.L. Liu, Angew. Chem. Int. Ed. 42 (2003) 3493.
[21] S.M. Gao, L.Y. Zhu, Y. Xie, X.B. Qian, Eur. J. Inorg. Chem. 3 (2004) 557.
[22] S. Ding, P. Lu, J.G. Zheng, X.F. Yang, F.L. Zhao, J. Chen, H. Wu, M.M. Wu, Adv. Funct. Mater. 17 (2007) 1879.
[23] J. Dinesh, M. Eswaramoorthy, C.N.R. Rao, J. Phys. Chem. C 111 (2007) 510.
[24] A.I. Hochbaum, R.K. Chen, R.D. Delgado, W.J. Liang, E.C. Garnett, M. Najarian, A. Majumdar, P.D. Yang, Nature 451 (2008) 163.
[25] L.Y. Wang, P. Li, Y.D. Li, Adv. Mater. 19 (2007) 3304.
[26] M.P. Zach, K.H. Ng, R.M. Penner, Science 290 (2000) 2120.
[27] Z. Zhong, Y. Fang, W. Lu, C.M. Lieber, Nanoletters 5 (2005) 1143.
[28] C.C. Hu, K.H. Chang, M.C. Lin, Y.T. Wu, Nanoletters 6 (2006) 2690.
[29] S.L. Xiong, B.J. Xi, C.M. Wang, G.C. Xi, X.Y. Liu, Y.T. Qian, Chem. Eur. J. 13 (2007) 7926.
[30] J.J. Carvajal, M. Aguilo, F. Diaz, J.C. Rojo, Chem. Mater. 19 (2007) 6543.
[31] Z. Yu, Z.M. Yang, S. Wang, Y. Jin, G. Liu, M. Gong, X.S. Sun, Chem. Vapor Depos. 11 (2005) 433.
[32] K.A. Bertness, A. Roshko, L.M. Mansfield, T.E. Harvey, N.A. Sanford, J. Cryst. Growth 300 (2007) 94.
[33] H.M. Kim, D.S. Kim, Y.S. Park, D.Y. Kim, T.W. Kang, K.S. Chung, Adv. Mater. 14 (2002) 991.
[34] W.Q. Han, P. Redlich, F. Ernst, M. Ruhle, Appl. Phys. Lett. 76 (2000) 652.
[35] L. Yang, C.S. Xue, C.M. Wang, H.X. Li, Nanotechnology 14 (2003) 50.
[36] B.D. Liu, Y. Bando, C.C. Tang, G.Z. Shen, D. Golberg, F.F. Xu, Appl. Phys. Lett. 88 (2006) 27.
[37] S.C. Hung, Y.K. Su, S.J. Chang, S.C. Chen, T.H. Fang, L.W. Ji, Physica E 28 (2005) 115.
[38] A.P. Purdy, S. Case, N. Muratore, J. Cryst. Growth 252 (2003) 136.
[39] S.Y. Bae, H.W. Seo, J. Park, H. Yang, J.C. Park, S.Y. Lee, Appl. Phys. Lett. 81 (2002) 126.
[40] S. Kikkawa, K. Nagasaka, T. Takeda, M. Bailey, T. Sakurai, Y. Miyamoto, J. Solid State Chem. 180 (2007) 1984.
[41] S. Cho, J. Lee, I.Y. Park, S. Kim, Jpn. J. Appl. Phys. 41 (2002) 5237.
[42] J.H. Yang, L.M. Qi, C.H. Lu, J.M. Ma, H.M. Cheng, Angew. Chem. Int. Ed. 44 (2005) 598.
[43] Q. Gong, X.F. Qian, P.L. Zhou, X.B. Yu, W.M. Du, S.H. Xu, J. Phys. Chem. C 111 (2007) 1935.
[44] J.J. Miao, T. Ren, L. Dong, J.J. Zhu, H.Y. Chen, Small 1 (2005) 802.
[45] C.Y. Wu, S.H. Yu, S.F. Chen, G.N. Liu, B.H. Liu, J. Mater. Chem. 16 (2006) 3326.
[46] M.A. Reshchikov, F. Shahedipour, R.Y. Korotkov, B.W. Wessels, M.P. Ulmer, J. Appl. Phys. 87 (2000) 3351.
[47] Z.C. Wu, C. Pan, T.W. Li, G.J. Yang, Y. Xie, Cryst. Growth Des. 7 (2007) 2454.
[48] Q.W. Chen, D.L. Zhu, C. Zhu, J. Wang, Y.G. Zhang, Appl. Phys. Lett. 82 (2003) 1018.